npj | quantum materials

Perspective

Published in partnership with Nanjing University

https://doi.org/10.1038/s41535-024-00638-2

Unconventional superconductivity near a nematic instability in a multi-orbital system

Kazi Ranjibul Islam ✉ & Andrey Chubukov ✉

We analyze superconductivity in a multi-orbital fermionic system near the onset of a nematic order, using doped FeSe as an example. We associate nematicity with spontaneous polarization between d_{xz} and d_{yz} orbitals. We derive pairing interaction, mediated by soft nematic fluctuations, and show that it is attractive, and its strength depends on the position on the Fermi surface. As the consequence, right at the nematic quantum-critical point (QCP), superconducting gap opens up at T_c only at special points and extends into finite arcs at $T < T_c$. In between the arcs the Fermi surface remains intact. This leads to highly unconventional behavior of the specific heat, with no jump at T_c and seemingly finite offset at $T = 0$. We discuss gap structure and pairing symmetry away from a QCP and compare nematic and spin-fluctuation scenarios. We apply the results to $FeSe_{1-x}S_x$ and $FeSe_{1-x}Te_x$.

It is widely believed that superconductivity in the cuprates, Fe-pnictides, heavy fermion, and other correlated electron systems is of electronic origin and at least in some portion of the phase diagram can be understood as mediated by soft fluctuations of a particle-hole order parameter, which is about to condense. The most studied scenario of this kind is pairing mediated by spin fluctuations. For the cuprates, it naturally leads to $d_{x^2-y^2}$ pairing. For Fe-pnictides, spin-mediated pairing interaction is attractive in both s-wave (s^{+-}) and $d_{x^2-y^2}$ channels. The argument, why pairing holds despite that the electron-electron interaction is repulsive, is the same in the two cases—antiferromagnetic spin fluctuations, peaked at momentum Q, increase the magnitude of a repulsive pairing interaction at the momentum transfer Q (the pair hopping from $(k, -k)$ to $k + Q, -k - Q$). A repulsive pair hopping allows for a solution for a gap function, which changes sign between Fermi points at k_F and $k_F + Q$. There is still a repulsion at small momentum transfer, which is detrimental to any superconductivity, and the bare Coulomb interaction is indeed larger at small momenta than at Q. However, when spin fluctuations are strong, a repulsion at Q gets stronger than at small momentum, and sign-changing superconducting gap does develop. This scenario has been verified by e.g., observation of a spin resonance peak below T_c[1–6]. Spin fluctuations were also identified as the source for spontaneous breaking of lattice rotational symmetry (nematicity) in Fe-pnictides, as nematicity there develops in the immediate vicinity of the stripe magnetic order with momenta $Q = (\pi, 0)$ or $(0, \pi)$. It has been argued multiple times[7–11]that spin fluctuations create an intermediate phase with a composite spin order, which breaks symmetry between $(\pi, 0)$ and $(0, \pi)$, but reserves $O(3)$ spin-rotational symmetry.

Situation is different, however, in bulk Fe-chalcogenide FeSe, which has been extensively studied in the last few years using various techniques. A pure FeSe develops a nematic order at $T_p \sim 85K$, and becomes superconducting at $T_c \sim 9K$. A nematic order decreases upon isovalent doping by either S or Te ($FeSe_{1-x}S_x$ and $FeSe_{1-x}Te_x$) and in both cases disappears at critical x_c (0.17 for S doping and 0.53 for Te doping). There is no magnetic order below T_p for any x.

The absence of magnetism lead to two conjectures: (i) that nematicity in FeSe is a $d-$ wave Pomeranchuk order, with order parameter bilinear in fermions, rather than a composite spin order, for which an order parameter is a 4-fermion operator[12], and (ii) that the origin of superconductivity may be different from the one in Fe-pnictides. On (i), there is a consistency between the Pomeranchuk scenario for nematicity and the data already in pure FeSe: a Pomeranchuk order parameter necessary changes sign between hole and electron pockets[13], consistent with the data[12,14–16], and the temperature dependence of nematic susceptibility, measured by Raman, is in line with the Pomeranchuk scenario[17–19]. On (ii), superconductivity in pure FeSe is likely still mediated by spin fluctuations[20–26], as evidenced by the correlation between NMR $1/T_1$ and superconducting T_c, the consistency between ARPES data on the gap anisotropy and calculations within spin fluctuation scenario, and the fact that a magnetic order does develop under pressure[27]. However, near and above critical x_c, magnetic fluctuations are far weaker[28,29], e.g., a magnetic order does not develop until high enough pressure. This strongly reduces the strength of spin-mediated pairing as the letter requires inter-pocket interaction (pair-hopping) to be enhanced by spin fluctuations to overcome intra-pocket repulsion[30]. It has been argued[31–35] based on a

School of Physics and Astronomy and William I. Fine Theoretical Physics Institute, University of Minnesota, Minneapolis, MN 55455, USA.
✉e-mail: islam074@umn.edu; achubuko@umn.edu

variety of data (see below) that superconductivity for such x is qualitatively different from the one in pure FeSe. One argument here is that the gap anisotropy changes sign, another is that T_c in $FeSe_{1-x}Te_x$ shows a clear dome-like behavior around x_c.

In this communication, we address the issue whether superconductivity in doped FeSe near x_c can be mediated by nematic fluctuations. It seems natural at first glance to replace spin fluctuations by soft nematic fluctuations as a pairing glue. However, there are two obstacles, both related to the fact that soft nematic fluctuations are at small momentum transfer. First, they do not affect the pair hopping term between hole and electron pockets, which is the key element for spin-mediated superconductivity. Second, the bare pairing interaction at small momentum transfer is repulsive, and dressing it by nematic fluctuations only makes the repulsion stronger.

We show that the pairing interaction $V_{\rm eff}(k,-k;p,-p)$, mediated by nematic fluctuations (first two momenta are incoming, last two are outgoing), does become attractive near x_c, however for a rather special reason, related to the very origin of the Pomeranchuk order. Namely, the driving force for a $d-$wave Pomeranchuk order is density-density interaction between hole and electron pockets. It does have a $d-$wave component $U^{\rm d}_{\rm he}$ because low-energy excitations in the band basis are constructed of d_{xz} and d_{yz} orbitals. A sign-changing nematic order (a spontaneous splitting of densities of d_{xz} and d_{yz} orbitals) develops[13] when $U^{\rm d}_{\rm he}$ exceeds d-wave intra-pocket repulsion, much like sign-changing s^{+-} order develops when pair hopping exceeds intra-pocket repulsion in the particle-particle channel. By itself, $U^{\rm d}_{\rm he}$ does not contribute to pairing, however taken at the second order, it produces an effective attractive interaction between fermion on the same pocket. We go beyond second order and collect all ladder and bubble diagrams which contain d-wave polarization bubbles at a small momentum transfer. We show that this induced attraction is proportional to the susceptibility for a $d-$wave Pomeranchuk order. Because a nematic susceptibility diverges at x_c, the induced attraction necessary exceeds the bare intra-pocket repulsion in some range around x_c, i.e., the full intra-pocket pairing interaction becomes attractive.

This attractive interaction $V_{\rm eff}(\mathbf{k},-\mathbf{k};,\mathbf{p},-\mathbf{p}) \propto A_{\mathbf{k},\mathbf{p}}\chi_{\rm nem}(|\mathbf{k}-\mathbf{p}|)$ is rather peculiar because it inherits from $U^{\rm d}_{\rm he}$ the $d-$wave form-factor $A_{\mathbf{k},\mathbf{p}} = \cos^2(\theta_{\mathbf{k}}+\theta_{\mathbf{p}})$, where $\theta_{\mathbf{k}}$ and $\theta_{\mathbf{p}}$ specify the location of the fermions ((in our case, this holds on the hole pocket, which is made equally out of d_{xz} and d_{yz} orbitals). A similar pairing interaction has been earlier suggested for one-band models on phenomenological grounds[36–39] assuming that $d-$wave nematic coupling is attractive. We show that such an interaction emerges in the model with purely repulsive interactions, once we add the pairing component, induced by inter-pocket density-density $U^{\rm d}_{\rm he}$.

Because $\chi_{\rm nem}(\mathbf{k}-\mathbf{p})$ diverges at $\mathbf{k}=\mathbf{p}$, the presence of the form-factor $A_{\mathbf{k},\mathbf{p}}$ in $V_{\rm eff}(\mathbf{k},-\mathbf{k};,\mathbf{p},-\mathbf{p})$ implies that the strength of the attraction depends on the position of a fermion on a Fermi surface. As the consequence, the gap function on the hole pocket is the largest around hot points, specified by $\theta_h = n\pi/2, n=0-3$, and rapidly decreases in cold regions centered at $\theta_c = n\pi/2+\pi/4, n=0-3$, This has been already emphasized in the phenomenological study[36]. This behavior shows up most spectacularly right at a nematic QCP, where the gap emerges at T_c only at hot spots and extends at smaller T into finite size arcs. The arcs length grows as T decreases, but as long as T is finite, there exist cold regions where the gap vanishes, i.e., the system preserves pieces of the original Fermi surface. At $T=0$, the gap opens everywhere except at the cold spots θ_c, where nematic form factor $\cos 2\theta$ vanishes, but is still exponentially small near them, $\Delta(\theta) \propto \exp -1/(\theta-\theta_c)^2$.

This, we argue, leads to highly unconventional behavior of the specific heat coefficient C_v/T, which does not display a jump at T_c and instead increases as $(T_c-T)^{1/2}$, passes through a maximum at $T\sim 0.8T_c$, and behaves at smaller T like there is a non-zero residual C_v/T at $T\to 0$ (see Fig. 2). In reality, C_v/T vanishes at $T=0$, but nearly discontinuously, as $1/(\log(T_c/T))^{1/2}$. Also, because the regions, where the gap is non-zero, are disconnected, the gap phases are uncorrelated, and $s-$wave, $d-$wave and two-component $p-$wave $(k_x+e^{i\alpha}k_y)$ states are degenerate.

At a finite distance from a QCP and/or in the presence of non-singular pair-hopping between hole and electron pockets, the gap function becomes continuous, but maxima at $\theta = n\pi/2$ remain. The specific heat coefficient $C(T)/T$ acquires a finite jump at T_c, but holds the same behavior at intermediate T as in Fig. 4, within some distance to a QCP. The condensation energies for $s-$wave, $d-$wave and $p-$wave states split. Which order develops depends on the interplay between the attractive pairing interaction, mediated by nematic fluctuations, and non-singular repulsion. The letter is far stronger in $s-$wave and $d-$wave channels, which favors $p-$wave symmetry. In this case, the most likely outcome is $k_x \pm ik_y$ state, which breaks time-reversal symmetry.

Results

Model

The electronic structure of pure/doped FeSe in the tetragonal phase consists of two non-equal hole pockets, centered at Γ, and two electron pockets centered at $X=(\pi,0)$ and $Y=(0,\pi)$ in the 1FeBZ. The hole pockets are composed of d_{xz} and d_{yz} fermions, the X pocket is composed of d_{yz} and d_{xy} fermions, and the Y pocket is composed of d_{xz} and d_{xy} fermions. The inner hole pocket is quite small and likely does not play much role for nematic order and superconductivity. We assume that heavy d_{xy} fermions also do not play much role and consider an effective two-orbital model with a single d_{xz}/d_{yz} circular hole pocket, and mono-orbital electron pockets (d_{yz} X-pocket and d_{xz} Y-pocket). We define fermionic operators for mono-orbital Y and X pockets as f_1 and f_2, respectively ($f_{1,\mathbf{k},\sigma} = d_{xz,\mathbf{k}+Y,\sigma}, f_{2,\mathbf{k},\sigma} = d_{yz,\mathbf{k}+X,\sigma}$). The band operator for the hole pocket is $h_{\mathbf{k},\sigma} = \cos\theta_{\mathbf{k}} d_{yz,\mathbf{k},\sigma} + \sin\theta_{\mathbf{k}} d_{xz,\mathbf{k},\sigma}$. The kinetic energy is quadratic in fermionic densities and there are 14 distinct C_4-symmetric interactions[40] involving low-energy fermions near the hole and the two electron pockets (see Supplementary Discussions I[41] for details). We take the absence of strong magnetic fluctuations in doped FeSe as an evidence that interactions at momentum transfer between Γ and X (Y) are far smaller than the interactions at small momentum transfer and neglect them. This leaves 6 interactions with small momentum transfer: 3 within hole or electron pockets and 3 between densities of fermions near different pockets. The single interaction between hole fermions contains an angle-independent term and terms proportional to $\cos 2\theta_{\mathbf{k}} \cos 2\theta_{\mathbf{p}}$ and $\sin 2\theta_{\mathbf{k}} \sin 2\theta_{\mathbf{p}}$, the two interactions between hole and electron pockets contain an angle-independent and a $\cos 2\theta_{\mathbf{k}}$ term, where $\mathbf{k}$ belongs to the hole pocket and the three interactions between fermions on electron pockets contain only angle-independent terms.

Nematic susceptibility

Like we said, we associate the nematic order with a d-wave Pomeranchuk order. In the orbital basis, this order is an orbital polarization (densities of d_{xz} and d_{yz} fermions split). In the band basis, we introduce two $d-$wave order parameters on hole and electron pockets: $\phi_{\rm h} = \sum_{\mathbf{k},\sigma}\langle h^\dagger_{\mathbf{k},\sigma} h_{\mathbf{k},\sigma}\rangle \cos 2\theta_{\mathbf{k}}$ and $\phi_{\rm e} = \sum_{\mathbf{k}}\langle f^\dagger_{2,\mathbf{k},\sigma} f_{2,\mathbf{k},\sigma}\rangle - \langle f^\dagger_{1,\mathbf{k}\sigma} f_{1,\mathbf{k},\sigma}\rangle$. The set of two coupled self-consistent equations for $\phi_{\rm h}$ and $\phi_{\rm e}$ is obtained by summing ladder and bubble diagrams (see Supplementary Discussions II[41]) and is

$$\begin{aligned} \phi_{\rm h} &= -\phi_{\rm h} U^{\rm d}_{\rm h} \Pi^d_h - \phi_{\rm e} U^{\rm d}_{\rm he} \Pi_e, \\ \phi_{\rm e} &= -\phi_{\rm e} U^{\rm d}_{\rm e} \Pi_e - 2\phi_{\rm h} U^{\rm d}_{\rm he} \Pi^d_h. \end{aligned} \quad (1)$$

Here, $\Pi^d_h = -\int G^h_p G^h_p \cos 2\theta_{\mathbf{p}}$, and $\Pi_e = -(1/2)\int_p \left(G^X_p G^X_p + G^Y_p G^Y_p\right)$ are the polarization bubbles for the hole and the electron pockets, ($G^i_p = G^i(p,\omega_m)$ are the corresponding Green's functions and $\int_p$ stands for $T\sum_{\omega_n}\int \frac{d^2\mathbf{p}}{(2\pi)^2}$). As defined, Π^d_h and Π_e are positive. The couplings $U^{\rm d}_{\rm h}$, $U^{\rm d}_{\rm e}$ and $U^{\rm d}_{\rm he}$ are $d-$wave components of intra-pocket and inter-pocket density-density interactions. All interactions are positive (repulsive). The analysis of (1) shows that the nematic order with different signs of $\phi_{\rm h}$ and $\phi_{\rm e}$ develops when $U^{\rm d}_{\rm he}$ is strong enough with the condition $2\left(U^{\rm d}_{\rm he}\right)^2 \geq U^{\rm d}_{\rm h} U^{\rm d}_{\rm e}$.

The nematic susceptibility is inversely proportional to the determinant of (1). Evaluating it at a small but finite momentum q, we obtain $\chi_{\rm nem}(q) \propto 1/$

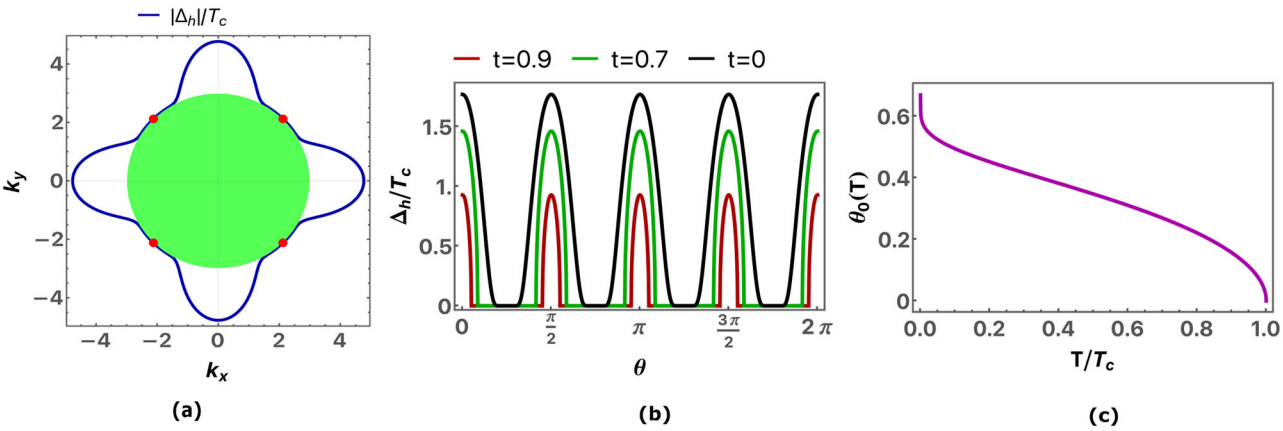

Fig. 1 | Superconductivity at the nematic QCP($\delta = 0$). a We plot the absolute value of the SC gap scaled by the transition temperature T_c, Δ_h/T_c(blue) on the hole pocket at zero temperature as a function of the angle on the Fermi surface(green disk) with radius 3 unit. The gap is exponentially small near the cold spots(red dots) while maximum along the k_x and k_y axis. In (**b**), we plot the angular variation of the gap, $|\Delta_h|/T_c$ on the hole pocket for three different reduced temperatures, $t = 0.9$, 0.7 and 0 below the transition point T_c. At finite temperature, the gap vanishes on the four patches of the Fermi surface arcs(flat segments of the gap). In (**c**), we plot the width of the gap, $\theta_0(T)$ as a function of the reduced temperature $t = T/T_c$. We keep the coupling strength $g = 1$ here.

Z, where

$$Z = \left(1 + U_{\rm h}^{\rm d}\,\Pi_h^d(q)\right)\left(1 + U_{\rm e}^{\rm d}\,\Pi_e(q)\right) - 2(U_{\rm he}^{\rm d})^2\Pi_h^d(q)\Pi_e(q). \quad (2)$$

Pairing interaction

Our goal is to verify whether the pairing interaction near the onset of a nematic order is (i) attractive, (ii) scales with the nematic susceptibility, and (iii) contains the d-wave form-factor $\cos^2(2\theta_{\mathbf{k}})$. To do this, we use the fact that $\chi_{\rm nem}(\mathbf{q})$ contains polarization bubbles $\Pi_h^d(\mathbf{q})$ and $\Pi_e(\mathbf{q})$, and obtain the fully dressed pairing interaction by collecting infinite series of renormalizations that contain $\Pi_h^d(\mathbf{q})$ and $\Pi_e(\mathbf{q})$ with small momentum $\mathbf{q}$. This can be done analytically (see refs. 41,42 for detail). Because $\mathbf{q}$ is small, the dressed pairing interactions are between fermions on only hole pocket or only electron pockets: $V_{\rm eff}^{\rm h}(\mathbf{k},\mathbf{q}) = V_{\rm eff}^{\rm h}(\mathbf{k}+\mathbf{q}/2, -(\mathbf{k}+\mathbf{q}/2); \mathbf{k}-\mathbf{q}/2, -(\mathbf{k}-\mathbf{q}/2))$, $V_{\rm eff}^{\rm e}(\mathbf{k},\mathbf{q}) = V_{\rm eff}^{\rm e}(\mathbf{k}+\mathbf{q}/2, -(\mathbf{k}+\mathbf{q}/2); \mathbf{k}-\mathbf{q}/2, -(\mathbf{k}-\mathbf{q}/2))$. We find

$$V_{\rm eff}^{\rm h}(\mathbf{k},\mathbf{q}) = \frac{U_h^d}{1 + U_h^d\Pi_h^d(\mathbf{q})} - A_h(U_{\rm he}^{\rm d})^2\cos^2 2\theta_{\mathbf{k}}\,\chi_{\rm nem}(\mathbf{q}) + \ldots \quad (3)$$

$$V_{\rm eff}^{e}(\mathbf{k},\mathbf{q}) = \frac{U_e^d}{1 + U_e^d\Pi_e(\mathbf{q})} - A_e(U_{\rm he}^{\rm d})^2\,\chi_{\rm nem}(\mathbf{q}) + \ldots, \quad (4)$$

where $A_h = \frac{\Pi_e}{1+U_{\rm h}^{\rm d}\Pi_h^d(\mathbf{q})}$ and $A_e = \frac{1}{2}\frac{\Pi_h^d}{1+U_{\rm e}^{\rm d}\Pi_e(\mathbf{q})}$. The dots stand for other terms which do not contain $\Pi_h^d(\mathbf{q})$ and $\Pi_e^d(\mathbf{q})$ and are therefore not sensitive to the nematic instability.

We see that each interaction contains two terms. The first is the dressed intra-pocket pairing interaction. It does get renormalized, but remains repulsive and non-singular at the nematic instability. The second term is the distinct interaction, induced by $U_{\rm he}^{\rm d}$. It is (i) attractive, (ii) scales with the nematic susceptibility, and (iii) contains the $d-$wave nematic form-factor $\cos^2 2\theta_{\mathbf{k}}$. We emphasize that the attraction is induced by inter-pocket density-density interaction, despite that relevant nematic fluctuations are with small momenta and the pairing interactions involve fermions from the same pocket.

Gap equation

Near a nematic QCP, $\chi_{\rm nem}(\mathbf{q})$ is enhanced and the interaction, induced by $U_{\rm he}^{\rm d}$, is the dominant one. In the absence of pair-hopping, the gap equation decouples between hole and electron pockets. The most interesting case is when the gap develops first on the hole pocket (the case $A_h > A_e$). We use Ornstein-Zernike form $\chi_{\rm nem}(\mathbf{q}) = \chi_0/(\delta^2 + q^2)$, where δ is the distance to a nematic QCP in units of momentum. At small δ, relevant q are of order δ. To first approximation, the non-linear equation for $\Delta_{\rm h}(\mathbf{k})$ then becomes local, with angle-dependent coupling:

$$1 = g\cos^2 2\theta_{\mathbf{k}}\int_0^\Lambda dx \frac{\tanh\left(\frac{\sqrt{x^2+|\Delta_{\rm h}(\mathbf{k})|^2}}{2T}\right)}{\sqrt{x^2+\Delta_{\rm h}(\mathbf{k})^2}}. \quad (5)$$

where $g = m(U_{\rm he}^{\rm d})^2\chi_0/(4\pi k_{\rm F}\delta)$. Because the coupling is larger at $\theta_{\mathbf{k}} = n\pi/2$, $n = 0-3$, the gap appears at $T_{\rm c} = 1.13\Lambda\exp(-1/g)$ only at these points. As T decreases, the range, where the gap is non-zero, extends to four finite arcs with the width $\theta_0(T) = 0.5\arctan\sqrt{g\log T_{\rm c}/T}$ (see Fig. 1c). In the areas between the arcs, the original Fermi surface survives. We emphasize that this is the original Fermi surface, not the Bogoliubov one, which could potentially develop inside the superconducting state[43,44]. We plot $|\Delta_{\rm h}(\mathbf{k})|$ along the Fermi surface at $T = 0$ and a finite T in Fig. 1a, b, and plot $\theta_0(T)$ as a function of $T/T_{\rm c}$ in Fig. 1c. The phases of the gap function in the four arcs are not correlated, hence $s-$wave, $d-$wave ($d_{x^2-y^2}$) and two-component $p-$wave ($k_{\rm x} + e^{i\alpha}k_{\rm y}$ with arbitrary α) are all degenerate. At $T = 0$, the arcs ends merge at $\theta_{\mathbf{k}} = n\pi/2 + \pi/4$, $n = 0-3$ and the gap becomes non-zero everywhere except these cold spots(red dots in Fig. 1a). In explicit form, $|\Delta_{\rm h}(k)| = 1.76T_{\rm c}\exp\{-\tan^2 2\theta_{\mathbf{k}}/g\}$. The gap near cold spots becomes a bit smoother if we keep the Landau damping in $\chi_{\rm nem}$ and solve the dynamical pairing problem, but still $\Delta_{\rm h}(\mathbf{k})$ remains highly anisotropic.

Specific heat

We split the specific heat coefficient $\gamma_{\rm c} = C_{\rm v}(T)/T$ into contributions from the gapped and ungapped regions of the Fermi surface: $\gamma_{\rm c}(T) = \gamma_{\rm c}^n(T) + \gamma_{\rm c}^s(T)$. The first term, $\gamma_{\rm c}^n(T) = \frac{8N_0\pi}{3}\left[\frac{\pi}{4} - \theta_0(T)\right]$ which at small T becomes: $\gamma_{\rm c}^n(T) \approx \frac{4N_0\pi}{3\sqrt{g\log T_{\rm c}/T}}$. It evolves almost discontinuously: vanishes at $T = 0$, but reaches 1/3 of the normal state value already at $T = 0.01T_{\rm c}$. We obtained $\gamma_{\rm c}^s(T)$ numerically and show the result for the full $\gamma_{\rm c}(T)$ in Fig. 2. We see that $\gamma_{\rm c}(T)$ does not jump at $T_{\rm c}$. Instead, it increases from its normal state value as $\sqrt{T_{\rm c} - T}$, passes through maximum at $T \approx 0.8T_{\rm c}$ and nearly linearly decreases at smaller T, apparently with a finite offset at $T = 0$. It eventually drops to zero at $T = 0$, but only at extremely small T, as $1/(\log T_{\rm c}/T)^{1/2}$. We emphasize that $\gamma_{\rm c}(T)$ is a function of a single parameter $T/T_{\rm c}$, i.e., the smallness of the range, where $\gamma_{\rm c}(T)$ drops, is purely numerical.

Away from a nematic QCP

At a finite δ, $s-$ wave, $d-$ wave, and $p-$ wave solutions for the gap function are no longer degenerate. If we keep only the interaction induced by U^{d}_{he} (the second term in (4)), we find that s-wave solution has the lowest condensation energy. We show the eigenvalues $\lambda_{s,p,d}$ and the gap functions in Fig. 3a, b. The gap function is smooth and finite for all angles, but remains strongly anisotropic up to sizable δ. We define the gap anisotropy α as the ratio of the gap function on the hole fermi surface at $\theta = \pi/4$($k_x - k_y$ axis) to $\theta = 0$(k_x axis): $\alpha = \Delta_h(\pi/4)/\Delta_h(0)$ and show its variation with the nematic mass parameter δ in Fig. 3c. The specific heat coefficient $\gamma_c(T)$ has a finite jump at T_c, whose magnitude increases with δ, yet the low temperature behavior remains nearly the same as at a QCP up to sizable δ (Fig. 4). If we consider the full pairing interaction in (3), situation may change as the first term in (3) has comparable repulsive $s-$ wave and $d-$ wave harmonics, but a much smaller $p-$ wave harmonic. As the consequence, $p-$ wave may become the leading instability. The condensation energy for a p-wave state is the lowest for $k_x + ik_y$ and $k_x - ik_y$ gap functions. A selection of one of these states breaks time-reversal symmetry.

Comparison with experiments

We argued in this work is that pairing in doped FeSe near a nematic QCP is mediated by nematic fluctuations rather than by spin fluctuations. This is generally consistent with the observations in refs. 31,32,34 of two distinct pairing states in pure FeSe and in doped $FeSe_{1-x}S_x$ and $FeSe_{1-x}Te_x$ at $x \geq x_c$. More specifically, one can distinguish between magnetic and nematic pairing scenarios by measuring the angular dependence of the gap along the hole d_{xz}/d_{yz} pocket. We argued that a nematic-mediated pairing gives rise to an anisotropic gap, with maxima along k_x and k_y directions. Within spin-fluctuation scenario, the gap $\Delta_h(k) = a + b\cos 4\theta$ is the largest along the diagonal directions $k_x \pm k_y$ ($b < 0$, see e.g., ref. 45). The angular dependence of the gap in pure and doped FeSe has been extracted from ARPES and STM data in ref. 23,46–50. For pure and weakly doped FeSe, an extraction of $\cos 4\theta$ dependence is complicated because superconductivity co-exists with long-range nematic order, in which case the gap additionally has $\cos 2\theta$ term due to nematicity-induced mixing of $s-$ wave and $d-$ wave components[24,51]. Still, the fits of the ARPES data in refs. 23,46 yielded a negative b, consistent with spin-fluctuation scenario. A negative b is also

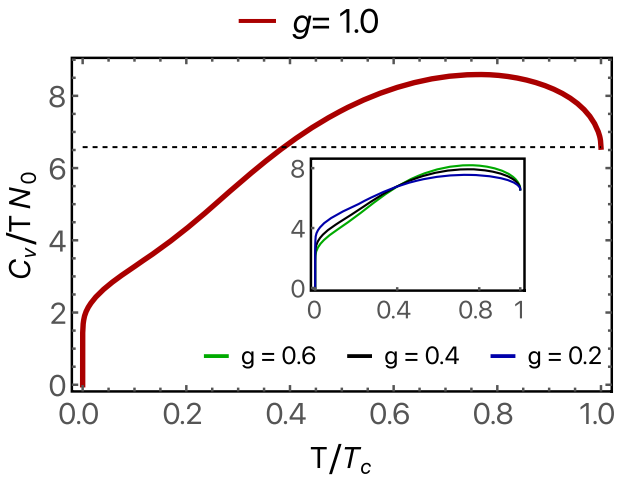

Fig. 2 | Specific heat at the nematic QCP($\delta = 0$). We plot the specific heat coefficient scaled by the density of state on Fermi surface, N_0 as a function of the reduced temperature, T/T_c for the coupling strength $g = 1.0$ in the main frame and for $g = 0.6$, 0.4 and 0.2 in the inset. The black dashed line represents the normal state contribution and is equal to $2\pi^2/3$.

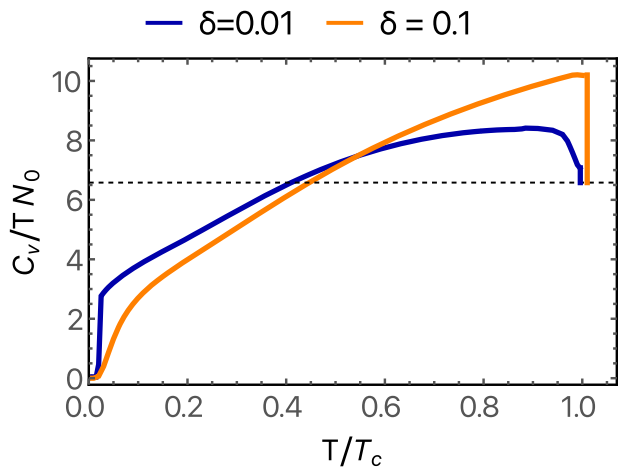

Fig. 4 | Specific heat away from the nematic QCP($\delta \neq 0$). We plot the variation of the specific heat coefficient scaled by the density of state on Fermi surface, N_0 with the reduced temperature T/T_c for a set of values of the nematic mass $\delta = 0.01$ and 0.1. Here, T_c is the superconducting transition temperature. The black dashed line represents the normal state contribution and is equal to $2\pi^2/3$. There is a finite specific heat jump at the transition point represented by the vertical line for both values of δ.

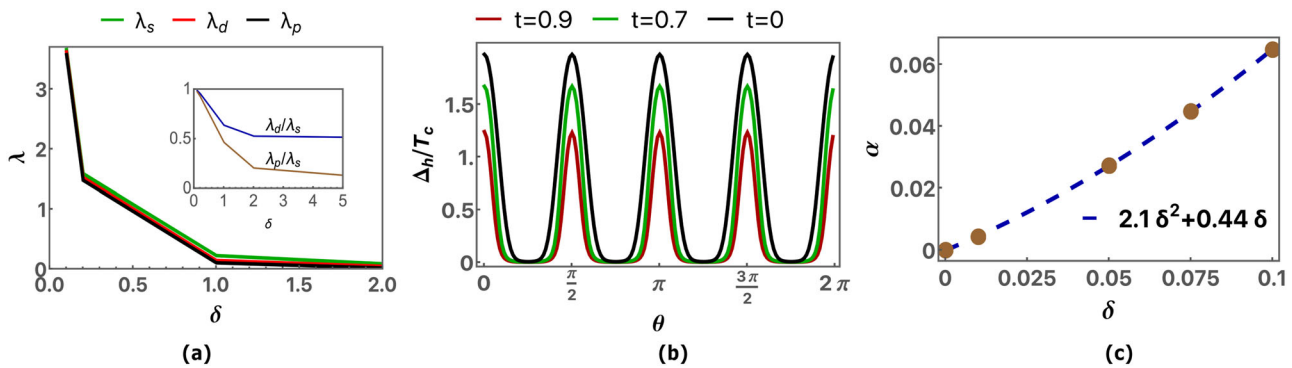

Fig. 3 | Superconductivity away from the nematic QCP($\delta \neq 0$). In (**a**), we plot the largest eigenvalue λ of the linearized gap equation defined in Supplementary Discussions VIII[41] in different angular momentum channels labeled as λ_s, λ_d and λ_p for the s, d and $p-$ wave respectively as a function of the nematic mass parameter δ. We show how the ratio of these eigenvalues vary with δ in the inset and find $\lambda_p/\lambda_s < \lambda_d/\lambda_s < 1$ which indicates that $s-$ wave is the leading instability. With δ going to zero, the ratios become closer to each other, indicating possible degeneracy among different pairing channels. In (b) we plot the angular variation(θ) of the gap function, $\Delta_h(\theta)/T_c$ on the hole pocket for a set of reduced temperatures, $t = T/T_c$ below the transition point T_c for $\delta = 0.01$. In (c) we plot the gap anisotropy $\alpha = \Delta_h(\theta = \pi/4)/\Delta_h(\theta = 0)$ as a function of the nematic mass δ and fit (blue dashed line) our result upto second order in δ with the fitting parameters $\alpha(\delta) = 2.12\,\delta^2 + 0.44\,\delta$.

consistent with the flattening of the gap on the hole pocket near $\theta = \pi$, observed in the STM study[47]. A negative prefactor for cos 4θ term was also reported for Fe-pnictides, e.g., $Ba_0.24K_{0.76}Fe_2As_2$, ref. 52. In contrast, gap maximum along k_y has been reported in a recent laser ARPES study of $FeSe_{0.78}S_{0.22}$ (ref. 48). Further, recent STM data for $FeSe_{0.81}S_{0.19}$ (ref. 49,50) detected a clear gap maxima along k_x and k_y. For Te-doped case, STM data for tetragonal $FeSe_{0.45}Te_{0.55}$ (ref. 53) also found the maximal gap along k_x and k_y directions, consistent with the pairing by nematic fluctuations. This STM data is in contradiction to earlier ARPES data for the same material, which reported a near-isotropic gap on the hole pocket[54]. However, the gap magnitude is only 2 meV, which calls for laser ARPES analysis. The gap anisotropy has also been analyzed in ref. 55, using angle-resolved specific heat data, but the authors of that work focused on the gap on the electron pockets. Taken together, these data strongly support the idea about different pairing mechanisms in pure FeSe and in doped ones at $x \geq x_c$, and are consistent with the change of the pairing glue from spin fluctuations at $x < x_c$ to nematic fluctuations at $x \geq x_c$.

Next, we argued that right at a nematic QCP, the gap vanishes in the cold regions on the Fermi surface, and this leads to highly unconventional behavior of the specific heat coefficient $\gamma_c(T)$. This holds when we neglect pair hopping between hole and electron pockets. In the presence of pair hopping, the gap becomes non-zero everywhere except, possibly, special symmetry-related points. Still, in the absence of magnetism nearby, pair-hopping is a weak perturbation, and the gap in cold regions is small. The specific heat of $FeSe_{1-x}S_x$ has been measured in refs. 33,56. The data clearly indicate that the jump of $\gamma_c(T)$ at T_c decreases with increasing x and vanishes at around x_c. At smaller T, $\gamma_c(T)$ passes through a maximum at around $0.8T_c$ and then decreases nearly linearly towards apparently a finite value at $T = 0$. The authors of ref. 31 argued that this behavior is not caused by fluctuations because residual resistivity does not exhibit a noticeable increase around x_c (ref. 57). Other experiments[58] also indicated that fluctuation effects get weaker with increasing x.

The behavior of $\gamma_c(T)$ around x_c was first interpreted as potential BCS-BEC crossover[32] and later as a potential evidence of an exotic pairing that creates a Bogolubov Fermi surface in the superconducting state[43,48,59]. We argue that the specific heat data are consistent with the nematic-mediated pairing, in which near x_c the gap develops in the arcs near k_x and k_y and nearly vanishes in between the arcs. This explanation is also consistent with recent observation[60] that superfluid density in $FeSe_{1-x}S_x$ drops at $x \geq x_c$, indicating that some fermions remain unpaired.

Finally, recent μSR experiments[60,61] presented evidence for time-reversal symmetry breaking in FeSe. The μSR signal is present below T_c for all x, however in $FeSe_{1-x}Te_x$ it clearly increases above x_c. This raises a possibility that the superconducting state at $x > x_c$ breaks time-reversal symmetry, at least in $FeSe_{1-x}Te_x$. Within our nematic scenario, this would indicate a $p-$wave pairing with $k_x \pm ik_y$ gap structure. We argued that $p-$wave pairing, mediated by nematic fluctuations, is a strong competitor to s^{+-} pairing.

There is one recent data set, which we cannot explain at the moment. Laser ARPES study of $FeSe_{0.78}S_{0.22}$ (ref. 48) detected superconducting gap in the polarizarion of light, which covers momenta near the X direction, but no gap in polarization selecting momenta near Y. Taken at a face value, this data implies that superconducting order strongly breaks C_4 symmetry. In our nematic scenario, pure k_x (or k_y) order is possible, but has smaller condensation energy than $k_x \pm ik_y$. More analysis is needed to resolve this issue.

Discussion

In this paper, we derived an effective pairing interaction near the onset of a nematic order in a 2D two-orbital/three band system of fermions and applied the results to doped FeSe. The model consists of a hole band, centered at Γ and made equally of d_{xz} and d_{yz} fermions, and two electron bands, centered at X and Y and made out of d_{yz} and d_{xz} fermions, respectively. The nematic order is a spontaneous polarization between d_{xz} and d_{yz} orbitals, which changes sign between hole and electron pockets. We found the pairing interaction as the sum of two terms: a dressed bare interaction, which remains non-singular and repulsive, and the term, induced by inter-pocket density-density interaction U^d_{he}. This last term contains the square of the nematic form-factor and scales with the nematic susceptibility, and is the dominant pairing interaction near the onset of a nematic order. We obtained the gap function and found that it is highly anisotropic with gap maxima along k_x and k_y directions. This is in variance with pairing by spin fluctuations, for which the gap has maxima along diagonal directions $k_x \pm k_y$. Right at the nematic QCP, the gap develops in four finite arcs around k_x and k_y, while in between the arcs the original Fermi surface survives. Such a gap function, degenerate between s-wave, $d-$wave, and $p-$wave, gives rise to highly unconventional behavior of the specific heat coefficient with no jump at T_c and seemingly finite value at $T = 0$ (the actual $C_v(T)/T$ vanishes at $T = 0$, but drops only at extremely low $T \sim 10^{-2}T_c$). In the tetragonal phase away from a QCP, the degeneracy is lifted, and there is a competition between $s-$wave and $k_x \pm ik_y$, the latter breaks time-reversal symmetry. In both cases, the gap remains strongly anisotropic, with maxima along X and Y directions. We compared our theory with existing experiments in some details.

Methods

Analytical calculations

Analytic calculations have been performed using diagrammatic theory. We obtained the susceptibility of the sign-changing d-wave nematic order by summing bubble and ladder series of diagrams for the renormalization of the nematic vertex, and obtained the pairing vertex by summing up ladder, bubble, and maximally crossed diagrams for the bare intra-pocket pairing interaction and for the pairing interaction induced by inter-pocket density-density interaction. We present the details of the calculations in Supplementary Discussion I–VIII.

Numerical calculations

We numerically solved the non-linear integral equation for the superconducting gap and used the results to compute the specific heat. The details are presented in the Supplementary Discussion VIII.

Data availability

The details of the analytical calculations are fully displayed in Supplementary Discussion I–VIII. Since this work did not require substantial numerical calculation, numerical data that are used in this study will be available upon the reasonable request from the first author.

Received: 27 October 2023; Accepted: 15 February 2024;
Published online: 15 March 2024

References

1. Christianson, A. et al. Unconventional superconductivity in $Ba_{0.6}K_{0.4}Fe_2As_2$ from inelastic neutron scattering. *Nat.* **456**, 930–932 (2008).
2. Lumsden, M. D. et al. Two-dimensional resonant magnetic excitation in $BaFe_{1.84}Co_{0.16}As_2$. *Phys. Rev. Lett.* **102**, 107005 (2009).
3. Chi, S. et al. Inelastic neutron-scattering measurements of a three-dimensional spin resonance in the FeAs-based $BaFe_{1.9}Ni_{0.1}As_2$ superconductor. *Phys. Rev. Lett.* **102**, 107006 (2009).
4. Inosov, D. et al. Normal-state spin dynamics and temperature-dependent spin-resonance energy in optimally doped $BaFe_{1.85}Co_{0.15}As_2$. *Nat. Phys.* **6**, 178–181 (2010).
5. Li, S. et al. Spin gap and magnetic resonance in superconducting $BaFe_{1.9}Ni_{0.1}As_2$. *Phys. Rev. B* **79**, 174527 (2009).
6. Parshall, D. et al. Spin excitations in $BaFe_{1.84}Co_{0.16}As_2$ superconductor observed by inelastic neutron scattering. *Phys. Rev. B* **80**, 012502 (2009).
7. Fernandes, R., Chubukov, A., Knolle, J., Eremin, I. & Schmalian, J. Preemptive nematic order, pseudogap, and orbital order in the iron pnictides. *Phys. Rev. B* **85**, 024534 (2012).
8. Fernandes, R., Chubukov, A. & Schmalian, J. What drives nematic order in iron-based superconductors? *Nat. Phys.* **10**, 97–104 (2014).

9. Fang, C., Yao, H., Tsai, W.-F., Hu, J. & Kivelson, S. A. Theory of electron nematic order in LaFeAsO. *Phys. Rev. B* **77**, 224509 (2008).
10. Xu, C., Müller, M. & Sachdev, S. Ising and spin orders in the iron-based superconductors. *Phys. Rev. B* **78**, 020501 (2008).
11. Fernandes, R. M., Orth, P. P. & Schmalian, J. Intertwined vestigial order in quantum materials: Nematicity and beyond. *Annu. Rev. Condens.* **10**, 133–154 (2019).
12. Chubukov, A. V., Khodas, M. & Fernandes, R. M. Magnetism, superconductivity, and spontaneous orbital order in iron-based superconductors: Which comes first and why? *Phys. Rev. X* **6**, 041045 (2016).
13. Xing, R.-Q., Classen, L. & Chubukov, A. V. Orbital order in FeSe: The case for vertex renormalization. *Phys. Rev. B* **98**, 041108 (2018).
14. Suzuki, Y. et al. Momentum-dependent sign inversion of orbital order in superconducting FeSe. *Phys. Rev. B* **92**, 205117 (2015).
15. Onari, S., Yamakawa, Y. & Kontani, H. Sign-reversing orbital polarization in the nematic phase of FeSe due to the C_2 symmetry breaking in the self-energy. *Phys. Rev. Lett.* **116**, 227001 (2016).
16. Benfatto, L., Valenzuela, B. & Fanfarillo, L. Nematic pairing from orbital-selective spin fluctuations in FeSe. *npj Quantum Mater.* **3**, 56 (2018).
17. Gallais, Y. & Paul, I. Charge nematicity and electronic Raman scattering in iron-based superconductors. *C R Phys* **17**, 113–139 (2016).
18. Udina, M., Grilli, M., Benfatto, L. & Chubukov, A. V. Raman response in the nematic phase of FeSe. *Phys. Rev. Lett.* **124**, 197602 (2020).
19. Klein, A., Lederer, S., Chowdhury, D., Berg, E. & Chubukov, A. Dynamical susceptibility of a near-critical nonconserved order parameter and quadrupole Raman response in Fe-based superconductors. *Phys. Rev. B* **98**, 041101 (2018).
20. Imai, T., Ahilan, K., Ning, F. L., McQueen, T. M. & Cava, R. J. Why does undoped FeSe become a high-T_c superconductor under pressure? *Phys. Rev. Lett.* **102**, 177005 (2009).
21. Glasbrenner, J. et al. Effect of magnetic frustration on nematicity and superconductivity in iron chalcogenides. *Nat. Phys.* **11**, 953–958 (2015).
22. Wang, Q. et al. Magnetic ground state of FeSe. *Nat. Commun.* **7**, 12182 (2016).
23. Liu, D. et al. Orbital origin of extremely anisotropic superconducting gap in nematic phase of FeSe superconductor. *Phys. Rev. X* **8**, 031033 (2018).
24. Hashimoto, T. et al. Superconducting gap anisotropy sensitive to nematic domains in FeSe. *Nat. Commun.* **9**, 282 (2018).
25. Classen, L., Xing, R.-Q., Khodas, M. & Chubukov, A. V. Interplay between magnetism, superconductivity, and orbital order in 5-pocket model for iron-based superconductors: Parquet renormalization group study. *Phys. Rev. Lett.* **118**, 037001 (2017).
26. Xing, R.-Q., Classen, L., Khodas, M. & Chubukov, A. V. Competing instabilities, orbital ordering, and splitting of band degeneracies from a parquet renormalization group analysis of a four-pocket model for iron-based superconductors: Application to FeSe. *Phys. Rev. B* **95**, 085108 (2017).
27. Sun, J. et al. Dome-shaped magnetic order competing with high-temperature superconductivity at high pressures in FeSe. *Nat. Commun.* **7**, 12146 (2016).
28. Wiecki, P. et al. Persistent correlation between superconductivity and antiferromagnetic fluctuations near a nematic quantum critical point in $FeSe_{1-x}S_x$. *Phys. Rev. B* **98**, 020507 (2018).
29. Ayres, J. et al. Transport evidence for decoupled nematic and magnetic criticality in iron chalcogenides. *Commun. Phys.* **5**, 100 (2022).
30. Mazin, I. I., Singh, D. J., Johannes, M. D. & Du, M. H. Unconventional superconductivity with a sign reversal in the order parameter of $LaFeAsO_{1-x}F_x$. *Phys. Rev. Lett.* **101**, 057003 (2008).
31. Hanaguri, T. et al. Two distinct superconducting pairing states divided by the nematic end point in $FeSe_{1-x}S_x$. *Sci. Adv.* **4**, eaar6419 (2018).
32. Shibauchi, T., Hanaguri, T. & Matsuda, Y. Exotic superconducting states in FeSe-based materials. *J. Phys. Soc. Jpn* **89**, 102002 (2020).
33. Sato, Y. et al. Abrupt change of the superconducting gap structure at the nematic critical point in $FeSe_{1-x}S_x$. *Proc. Natl. Acad. Sci.* **115**, 1227–1231 (2018).
34. Ishida, K. et al. Pure nematic quantum critical point accompanied by a superconducting dome. *Proc. Natl. Acad. Sci.* **119**, e2110501119 (2022).
35. Mukasa, K. et al. Enhanced superconducting pairing strength near a pure nematic quantum critical point. *Phys. Rev. X* **13**, 011032 (2023).
36. Lederer, S., Schattner, Y., Berg, E. & Kivelson, S. A. Enhancement of superconductivity near a nematic quantum critical point. *Phys. Rev. Lett.* **114**, 097001 (2015).
37. Schattner, Y., Lederer, S., Kivelson, S. A. & Berg, E. Ising nematic quantum critical point in a metal: A Monte Carlo study. *Phys. Rev. X* **6**, 031028 (2016).
38. Lederer, S., Schattner, Y., Berg, E. & Kivelson, S. A. Superconductivity and non-fermi liquid behavior near a nematic quantum critical point. *Proc. Natl. Acad. Sci.* **114**, 4905–4910 (2017).
39. Klein, A. & Chubukov, A. Superconductivity near a nematic quantum critical point: Interplay between hot and lukewarm regions. *Phys. Rev. B* **98**, 220501 (2018).
40. Fernandes, R. M. & Chubukov, A. V. Low-energy microscopic models for iron-based superconductors: a review. *Rep. Prog. Phys.* **80**, 014503 (2016).
41. See Supplementary material.
42. Dong, Z., Chubukov, A. V. & Levitov, L. Transformer spin-triplet superconductivity at the onset of isospin order in bilayer graphene. *Phys. Rev. B* **107**, 174512 (2023).
43. Setty, C., Bhattacharyya, S., Cao, Y., Kreisel, A. & Hirschfeld, P. Topological ultranodal pair states in iron-based superconductors. *Nat. Commun.* **11**, 523 (2020).
44. Setty, C., Cao, Y., Kreisel, A., Bhattacharyya, S. & Hirschfeld, P. Bogoliubov fermi surfaces in spin-$\frac{1}{2}$ systems: Model Hamiltonians and experimental consequences. *Phys. Rev. B* **102**, 064504 (2020).
45. Graser, S. et al. Spin fluctuations and superconductivity in a three-dimensional tight-binding model for $BaFe_2As_2$. *Phys. Rev. B* **81**, 214503 (2010).
46. Xu, H. et al. Highly anisotropic and twofold symmetric superconducting gap in nematically ordered $FeSe_{0.93}Te_{0.07}$. *Phys. Rev. Lett.* **117**, 157003 (2016).
47. Sprau, P. O. et al. Discovery of orbital-selective cooper pairing in FeSe. *Science* **357**, 75–80 (2017).
48. Nagashima, T. et al. Discovery of nematic bogoliubov fermi surface in an iron-chalcogenide superconductor. Preprint at https://doi.org/10.21203/rs.3.rs-2224728/v1 (2022).
49. Walker, M. et al. Electronic stripe patterns near the fermi level of tetragonal Fe(Se,S). *npj Quantum Mater* **8**, 60 (2023).
50. Da Silva Neto, E. et al. Superconductivity mediated by nematic fluctuations in tetragonal $FeSe_{1-x}S_x$. *Bulletin of the American Physical Society* (2024).
51. Kushnirenko, Y. et al. Three-dimensional superconducting gap in FeSe from angle-resolved photoemission spectroscopy. *Phys. Rev. B* **97**, 180501 (2018).
52. Ota, Y. et al. Evidence for excluding the possibility of *d*-wave superconducting-gap symmetry in Ba-doped KFe_2As_2. *Phys. Rev. B* **89**, 081103 (2014).
53. Sarkar, S. et al. Orbital superconductivity, defects, and pinned nematic fluctuations in the doped iron chalcogenide $FeSe_{0.45}Te_{0.55}$. *Phys. Rev. B* **96**, 060504 (2017).
54. Miao, H. et al. Isotropic superconducting gaps with enhanced pairing on electron fermi surfaces in $FeTe_{0.55}Se_{0.45}$. *Phys. Rev. B* **85**, 094506 (2012).

55. Zeng, B. et al. Anisotropic structure of the order parameter in $FeSe_{0.45}Te_{0.55}$ revealed by angle-resolved specific heat. *Nat. Commun.* **1**, 112 (2010).
56. Mizukami, Y. et al. Unusual crossover from bardeen-cooper-schrieffer to bose-einstein-condensate superconductivity in iron chalcogenides. *Commun. Phys.* **6**, 183 (2023).
57. Hosoi, S. et al. Nematic quantum critical point without magnetism in $FeSe_{1-x}S_x$ superconductors. *Proc. Natl. Acad. Sci.* **113**, 8139–8143 (2016).
58. Coldea, A. I. et al. Evolution of the low-temperature fermi surface of superconducting $FeSe_{1-x}S_x$ across a nematic phase transition. *npj Quantum Mater* **4**, 2 (2019).
59. Agterberg, D., Brydon, P. & Timm, C. Bogoliubov fermi surfaces in superconductors with broken time-reversal symmetry. *Phys. Rev. Lett.* **118**, 127001 (2017).
60. Matsuura, K. et al. Two superconducting states with broken time-reversal symmetry in $FeSe_{1-x}S_x$. *Proc. Natl. Acad. Sci.* **120**, e2208276120 (2023).
61. Roppongi, M. et al. in preparation.

Acknowledgements

We acknowledge with thanks useful conversations with D. Agterberg, E. Berg, P. Canfield, P. Coleman, Z. Dong, R. Fernandes, Y. Gallais, E. Gati, T. Hanaguri, P. Hirschfeld, B. Keimer, A. Klein, H. Kontani, L. Levitov, A. Pasupathi, I. Paul, A. Sacuto, J. Schmalian, T. Shibauchi, and R. Valenti. K. R. I would like to thank Shang-Shun Zhang for helping in the numerical study of the gap equation in the initial phase of the project. This work was supported by U.S. Department of Energy, Office of Science, Basic Energy Sciences, under Award No. DE-SC0014402.

Author contributions

All authors contributed equally to this work.

Competing interests

The authors declare no competing interests.

Additional information

Supplementary information The online version contains supplementary material available at https://doi.org/10.1038/s41535-024-00638-2.

Correspondence and requests for materials should be addressed to Kazi Ranjibul Islam or Andrey Chubukov.